Electronic Supplementary Material (ESI) for Energy & Environmental Science.

Supporting Information

Interpretation and Evolution of Open-Circuit Voltage, Recombination, Ideality Factor and Subgap Defect States during Reversible Light-Soaking and Irreversible Degradation of Perovskite Solar Cells

Wolfgang Tress[1,2*], Mozhgan Yavari[2], Konrad Domanski[1], Pankaj Yadav[1], Bjoern Niesen[3], Juan Pablo Correa Baena[4], Anders Hagfeldt[2], Michael Graetzel[1]

[1]Laboratory for Photonics and Interfaces, Institute of Chemical Sciences, Engineering, École Polytechnique Fédérale de Lausanne, 1015 Lausanne, Switzerland

[2]Laboratory of Photomolecular Science, Institute of Chemical Sciences and Engineering, École Polytechnique Fédérale de Lausanne, 1015 Lausanne, Switzerland.

[3]Photovoltaics and Thin-Film Electronics Laboratory, Institute of Microengineering, École Polytechnique Fédérale de Lausanne, 2002 Neuchâtel, Switzerland

[4]Massachusetts Institute of Technology, Cambridge, MA 02139, USA

*wolfgang.tress@epfl.ch

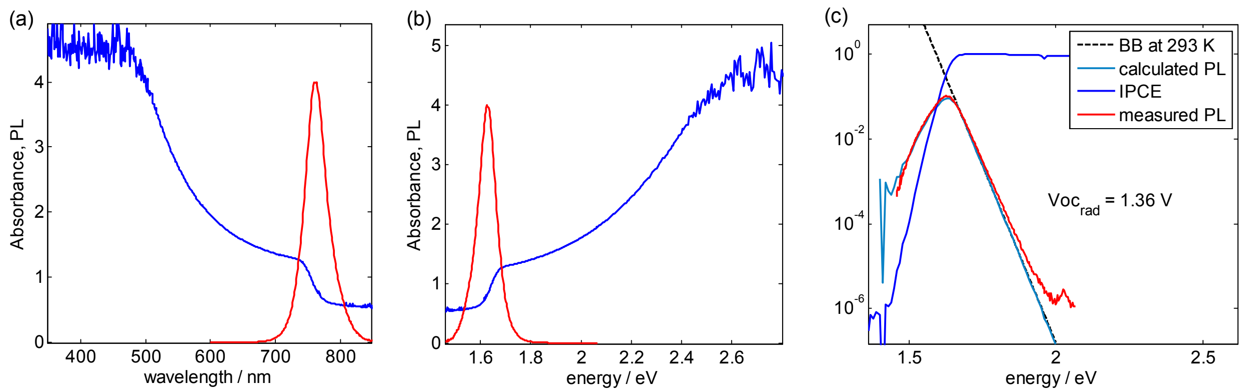

Figure SI1 (a) Absorbance, measured in transmission, not corrected for scattering and reflection, PL counts measured at an excitation wavelength of 450 nm. (b) The same data as a function of energy. (c) Normalized IPCE, comparison between predicted (cyan) and measured (red) PL emission spectrum. Absorbance and PL were measured at a film on glass, the IPCE of a meso TiO_2 device.

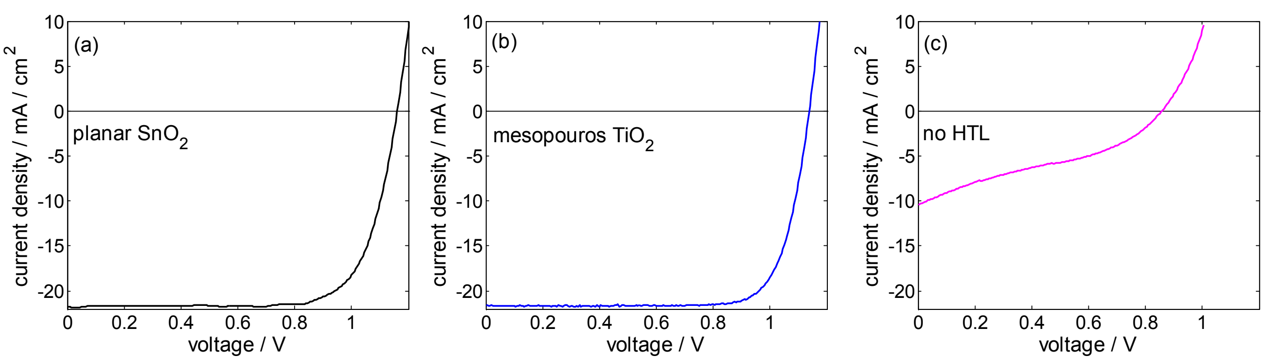

Figure SI2 *JV* curves of devices measured under solar simulator using a sweep rate of -10 mV/s and an aperture with an area of 0.16 cm^2 (electrode area 0.25 cm^2). (a) planar SnO_2 based device; (b) mesoporous TiO_2 based device; (c) device without HTL.

Table SI1 *JV* parameters of the devices shown in Fig. SI2.

	J_{sc} / mA/cm²	**V_{oc} / V**	**FF**	**PCE**	**Intensity / sun**
Planar SnO_2	21.7	1.16	0.75	19.7%	0.96
Mesoporous TiO_2	21.6	1.14	0.78	19.6%	0.98
Without HTL	10.4	0.86	0.34	3.0%	1

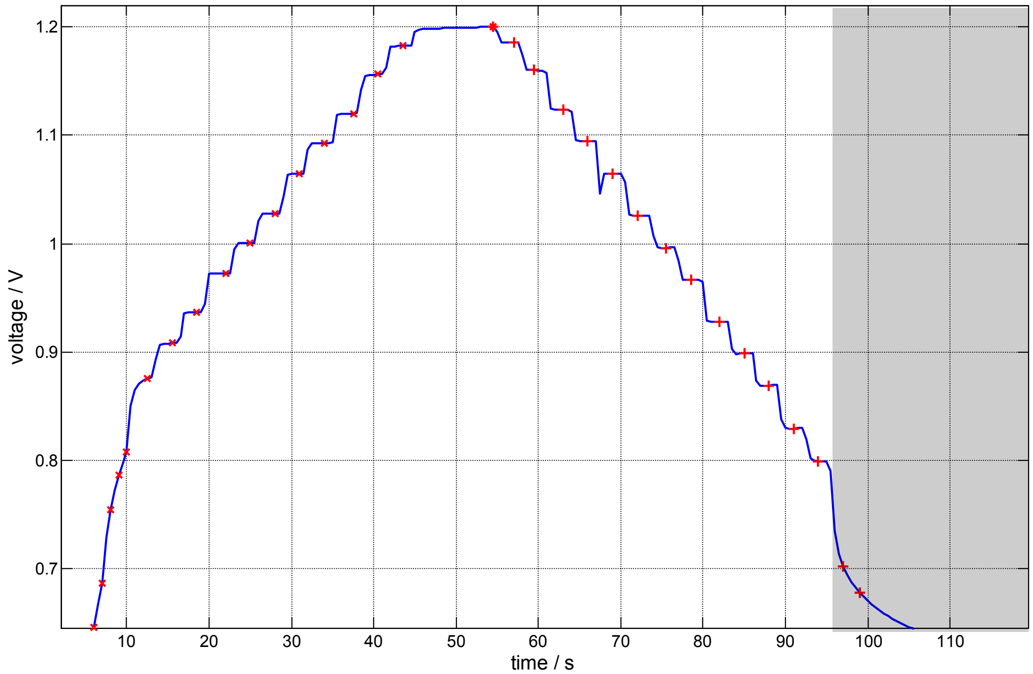

Figure SI3 Example of V_{oc} monitoring during an intensity sweep (planar device at 20ºC), where the intensity is swept up to 1.5 suns and back, taking three points per decade at 1, 2, and 5 (dwell time 3 s, 10 s at the maximum intensity). The symbols indicate the automatically detected voltage used for the light intensity dependent V_{oc} analysis in the paper. This approach is a trade-off and is not perfect as can be seen e.g. at the start of the sweep. Analyzing upward and downward scan increases the credibility of the data and allows to exclude a strong dependence on preconditioning. This approach is selected because waiting for V_{oc} to stabilize is not feasible due to light-soaking effects, which are separately studied in this work.

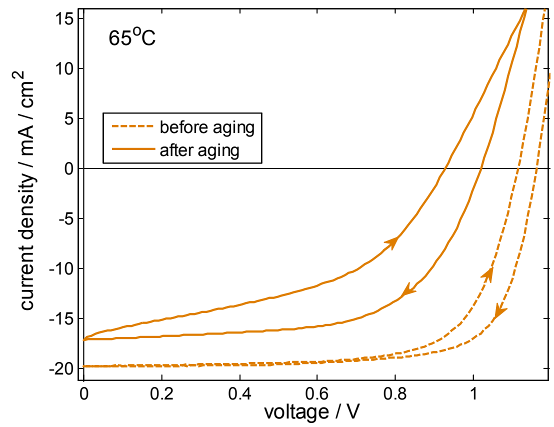

Figure SI4 *JV* loop of "aged meso-TiO_2" device measured at 65°C with 100 mV/s starting at 1.2 V. Aging was performed under 1 sun equivalent LED illumination at 65°C under N_2 for 8 days.

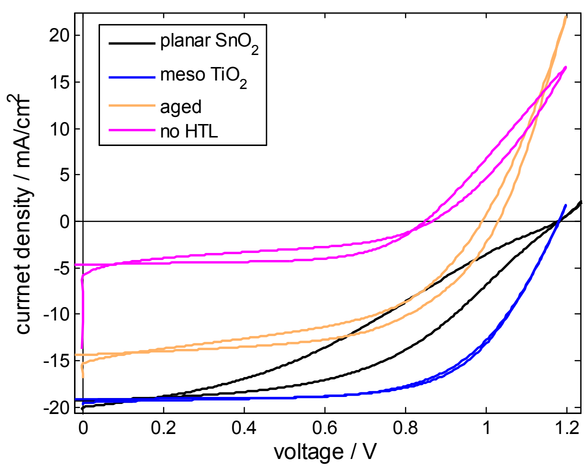

Figure SI5 *JV* curves of investigated devices measured with 10 mV/s starting at 0 V at 20°C under 1 sun equivalent LED illumination.

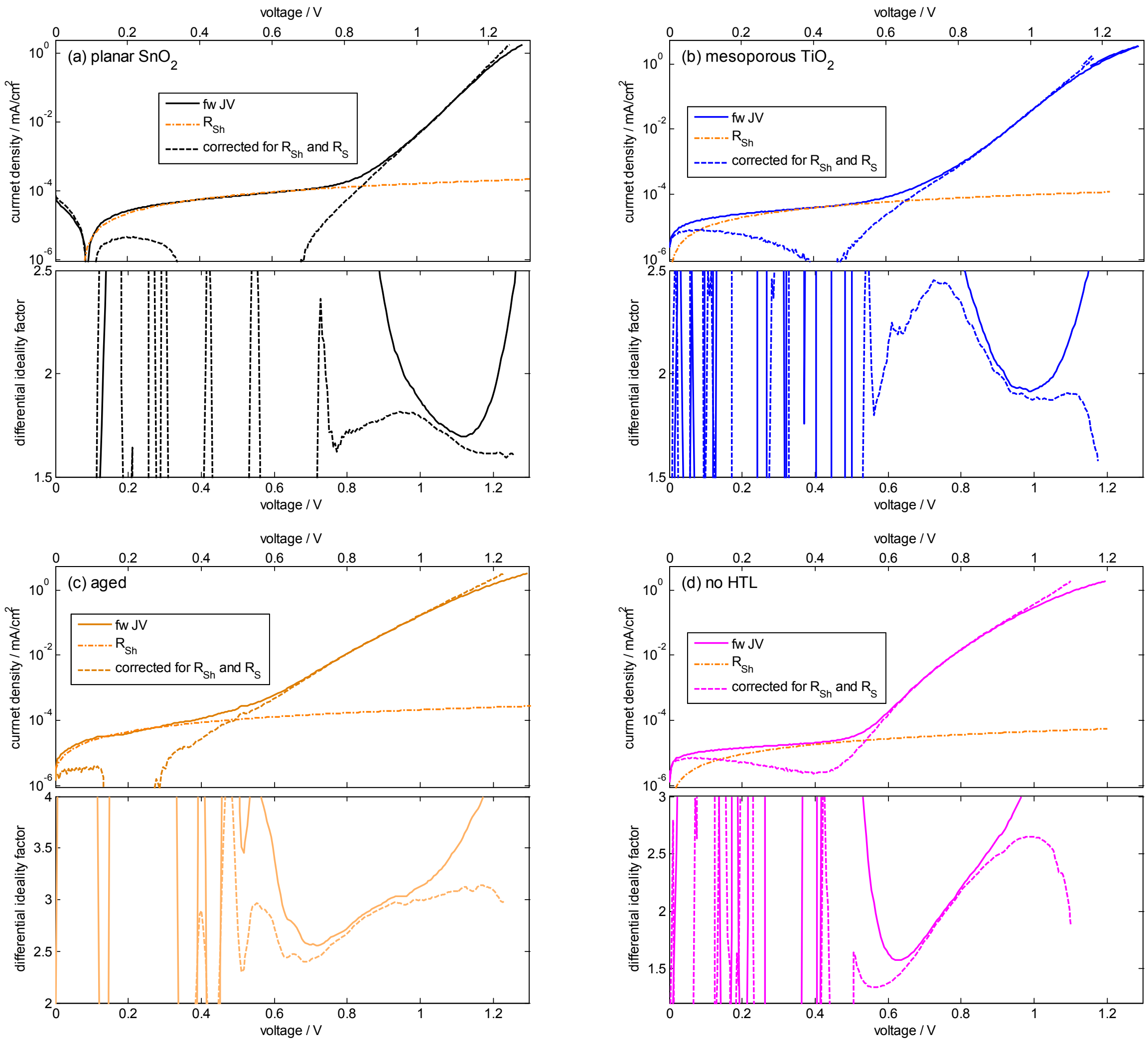

Figure SI6 Correction for parasitic resistances according to an equivalent circuit model: $I = I_0 \exp\left(\frac{e(V - IR_S)}{n_{ID} k_B T} - 1\right) + \frac{V - IR_S}{R_{Sh}}$. The corrected *JV* curves (dashed) were obtained in several steps: First, a linear fit of the experimental *JV* curve for small voltages (dash-dotted yellow line) to quantify the current flowing through the shunt resistance R_{Sh}. This curve is subtracted from the experimental curve. Second, the voltage was corrected by removing the linear contribution to the *JV* curve for high voltages ($V_{diode} = V - IR_S$). The differential ideality factor is plotted in the bottom panels showing that the correction (dashed) only slightly improves the reliability of the obtained value for n_{ID}.

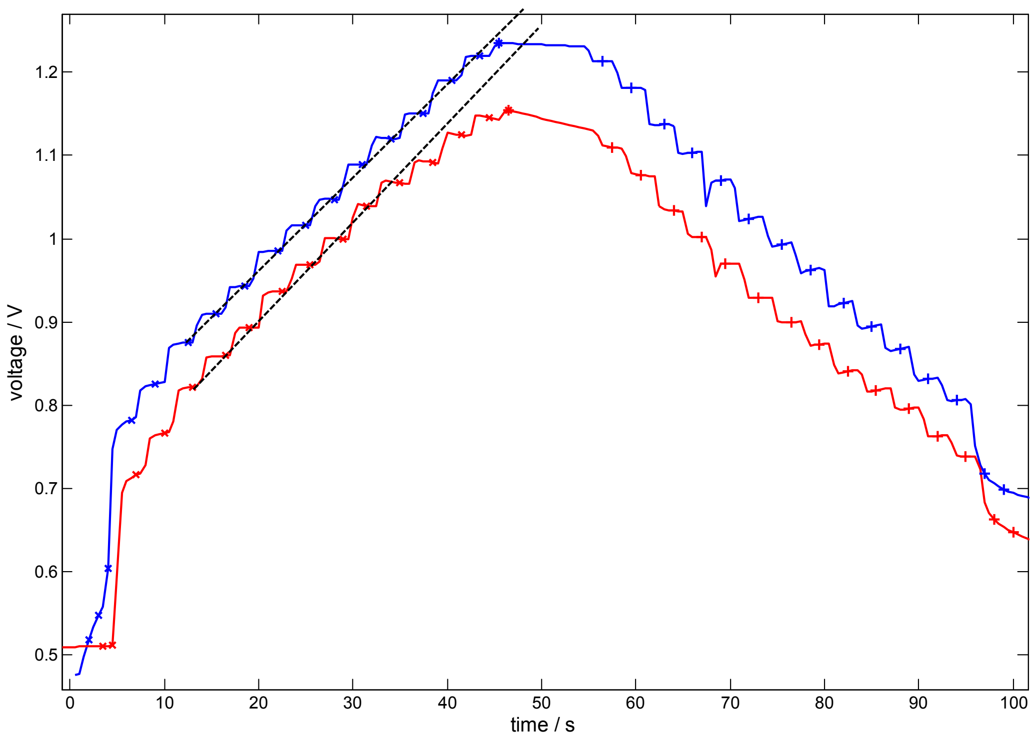

Figure SI7 V_{oc} monitoring during a stepwise sweep for a rather unstable meso-TiO_2 device (blue at 20^{o}C, red at 50^{o}C). In particular for high light intensities and temperatures, V_{oc} is already instable (albeit reversible) during the measurement procedure. These transients are to be considered when analyzing temperature dependent data at high light intensity and elevated temperatures in Fig. 7 of the main manuscript.

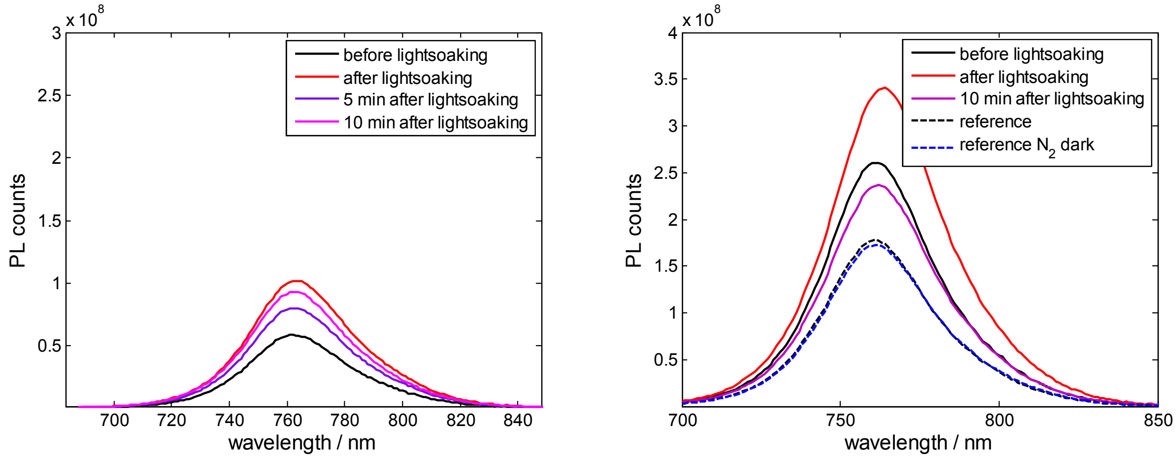

Figure SI8 PL spectra of perovskite films on glass upon light soaking for 2 hours, which was done in the same setup as the device characterization, i.e. in N_2 atmosphere under 1 sun equivalent LED illumination. The perovskite films were covered by a PMMA film to reduce the effect of atmosphere during storage and PL measurements. Data of two light-soaked samples are shown and one reference kept in the dark.

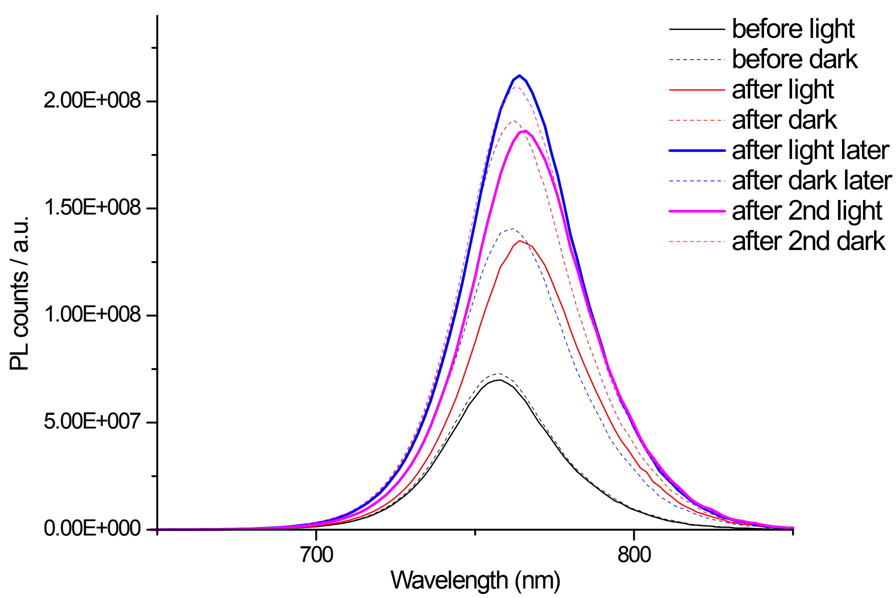

Figure SI9 PL spectra of two perovskite films on glass and covered with PMMA, one kept in the dark (dashed) and one under light (solid lines) for 2 hours, both in N_2 atmosphere. The PL slightly increases after storage in N_2 independent of illumination for this sample. Repeating the PL measurements 30 minutes later (films kept in the dark at ambient) changes the PL again slightly. A second round does as well. We conclude that the change of PL in these films is not clearly correlated to illumination.

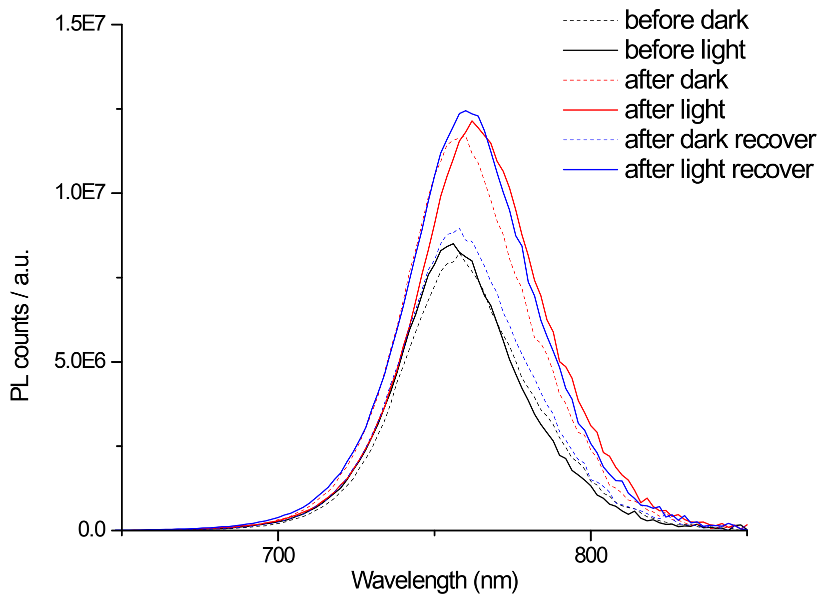

Figure SI10 PL spectra of two perovskite films on FTO/TiO_2 and covered with PMMA, one kept in the dark (dashed) and one under light (solid), cf. Fig. SI9. The absolute signal is by a factor of 10 quenched compared to the film on glass due to charge transfer and recombination at the TiO_2 interface. The trend of slightly increased PL upon storage in N_2 independent of illumination is maintained.

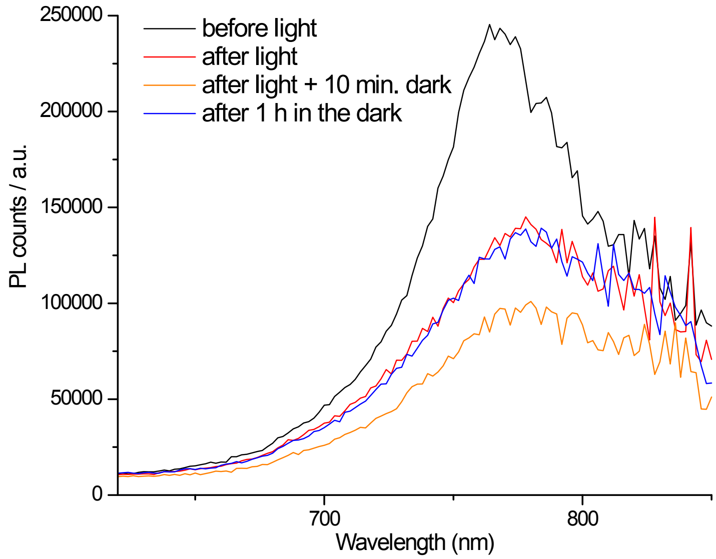

Figure SI11 PL spectra of a perovskite solar cell. The PL is measured through the glass substrate and the signal is much weaker compared to the films. The trend is inverted and fits the behavior of the open-circuit voltage, which decreased after light soaking and increases again after a rest in the dark.

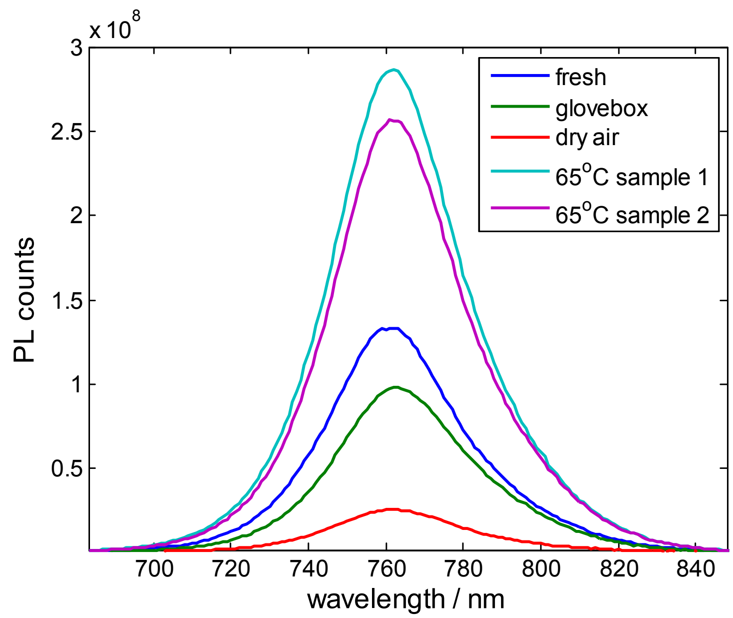

Figure SI12 PL of perovskite films on glass and covered with PMMA. Aging was performed for 8 days, either in an N_2 glovebox at ambient temperature (30 °C), under dry air (2…5 % RH), or on a hot plate in an N_2 glovebox. The PL was collected in an unmodified geometry of the spectroscopy setup in all cases and on films with the same thickness (excitation at 450 nm) allowing for a comparison of absolute spectra. In contrast to the aging behavior of devices, elevated temperatures do not lead to an increase in non-radiative recombination. The emission yield is even slightly increased indicating an annealing effect (whereas storage in the dark under non-inert atmosphere leads to a reduced emission yield).

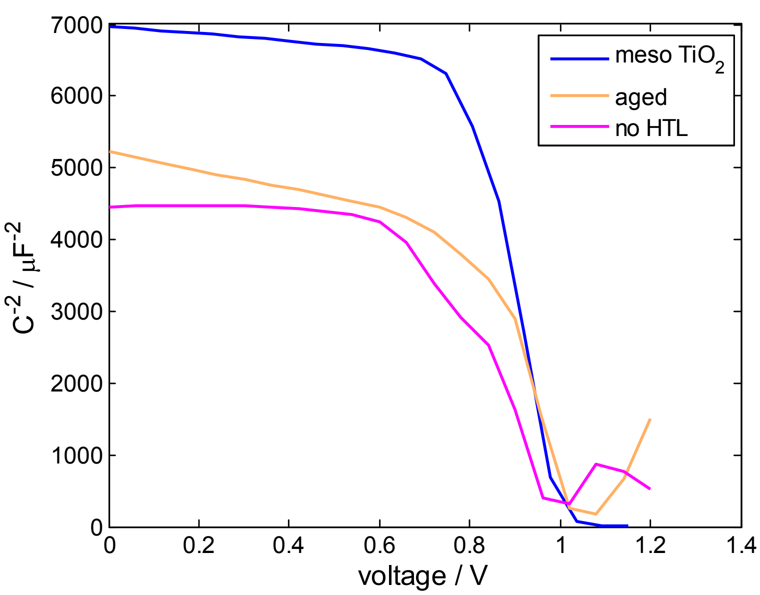

Figures SI13 Mott Schottky analysis. The extracted doping densities are 1.2×10^{16} cm^{-3} for the meso-TiO_2 device, 1.7×10^{16} cm^{-3} for the degraded one, and 3×10^{16} cm^{-3} for the device without HTL. The data was extracted at a frequency of 20 kHz.